Bulletin of the Seismological Society of America, Vol. 92, No. 2, pp. 854–862, March 2002

Dilatancy-Induced *P* Waves as Evidence for Nonlinear Soil Behavior

by I. Loukachev, N. Pralle, and G. Gudehus

Abstract A much-discussed topic in seismology deals with how and under which loading conditions soil shows nonlinear behavior and how this can be verified from seismograms. Seismologists have been seriously searching for signatures of nonlinear soil response to earthquakes for about two decades. A mechanism explaining the dispersion in the *P*-wave spectra due to the interaction between compressional (*P*) and shear (*S*) waves is presented. Shear waves in granular materials induce longitudinal dilatancy waves (so-called Δ waves) with approximately double frequency. This can be explained with dilatancy and contractancy, which is characteristic of granulates under shear deformations. The predicted dispersion is observed in laboratory experiments and verified by comparing accelerograms from hard-rock and soil stations from the Vrancea region, Romania. The arrival-time difference between Δ waves and *S* waves may theoretically be indicative of the thickness of nonsaturated granular layers. These results, modeled with nonlinear constitutive relations of the rate type, show a specific type of nonlinearity in granular sediments also for earthquakes of moderate magnitudes.

Introduction

Geotechnical engineers, who gathered a wealth of evidence for all types of soils under different quasistatic and dynamic loading conditions through laboratory experiments (e.g. Terzaghi, 1925; Bernatzik, 1947), have long known that soil is a nonlinear material. However, geoscientists, most prominently seismologists dealing with the subsurface response during earthquake shaking, have only implemented nonlinearity in their geological and geophysical models for soft sediments in the last 10–15 yr. Nonlinear soil behavior was verified by analyzing seismograms with several techniques. Other verification efforts were based on induced seismicity through seismic vibrators (Beresnev *et al.,* 1986; Beresnev and Nikolaev, 1988; Nikolaev, 1988). The research on nonlinear soil behavior during earthquakes has produced a wealth of literature since it is of importance for the microzonation of sites vulnerable to earthquakes. Most often, nonlinearity is synonymously used for shear modulus degradation during large strains (e.g., Bard, 1994; Beresnev *et al.,* 1994, 1995; Beresnev and Wen, 1995; Beresnev *et al.,* 1998), also termed deamplification. Amplification, however, of seismic-wave amplitudes are particularly observed in the upper layers of soft sediments, which is incorrectly attributed to the low velocity of those layers (Beresnev *et al.,* 1998). It is not because the nonlinearity reduces the wave velocity that amplification takes place, but because the grain pressure decreases with decreasing depth, which controls shear and bulk moduli and in consequence shear-wave velocity. Amplification, deamplification, and wave-propagation velocities depend on the local geologic conditions (i.e., whether seismic-wave paths lead through soft or stiff, loose or dense soilsor through cohesive or noncohesive formations) and on the frequency content and displacement amplitude of the propagating wave that determines the hysteretic behavior (Jarpe *et al.,* 1988; Chin and Aki, 1991; Darragh and Shakal, 1991; Aki, 1993; Beresnev and Wen, 1996; Sato *et al.,* 1996; Studer and Koller, 1997; Field *et al.,* 1998; Suetomi and Yoshida, 1998; Dimitriu *et al.,* 1999; Dimitriu *et al.,* 2000) and have been numerically modeled (Yu *et al.,* 1992). One important aspect has been whether soil behavior during a strong earthquake can be derived from weak-motion data, an endeavor that has been shown not to be advisable (Bolt, 1995).

However, the quest for signatures of nonlinear soil behavior in earthquake data has unveiled other phenomena. An extreme case of nonlinear soil behavior is highly significant to foundation engineers and can be attributed to the category of deamplification with regard to shear-wave propagation: the property of nearly and fully saturated sands to liquefy during undrained shear produces an excess pore water pressure increase and subsequently a drastic reduction of grain pressure (Terzaghi and Peck, 1967; Castro, 1969), which significantly reduces the shear modulus (Drnevich, 1972; Sato *et al.,* 1996; Pease and O'Rourke, 1997; Suetomi and Yoshida, 1998) and hence shear-wave amplitude (Loukachev *et al.,* 2000; Yang *et al.,* 2000; Gudehus *et al.,* 2001). Very loose soils can even completely liquefy, that is, the soil turns into a suspension allowing large deformations, hence inhibiting any shear-wave propagation (Loukachev, 2002).

Another manifestation of nonlinear soil behavior is the observation of higher harmonics in the frequency spectra. Several authors report on this nonlinear soil property based on studies using seismic vibrators (Beresnev *et al.,* 1986; Beresnev and Nikolaev, 1988; Nikolaev, 1988), which seems to be controversial (Solovev, 1990). The generation of higher harmonics can mathematically be described using elastic nonlinear constitutive equations (Heitz and Sánchez-Sesma, 1989). In this case, owing to the nonlinearity, a wave with frequency f induces waves with a peak frequency $2f$, which itself generates waves with a peak frequency of $4f$, and so on. As the base of a soil layer is excited with only one frequency f, the near-surface-wave motion will show a frequency spectra with higher harmonics $2f$, $4f$, and so on. However, this effect does disperse the seismic-wave spectra for the same wave component. Johnson *et al.* (1987) recognized a nonlinear interaction of elastic waves in a heterogeneous (crystalline) rock material but did not suggest any mechanisms to explain the observation. Belyakov *et al.* (1996) attributed acoustic nonlinear processes in rock to its structure and texture, its rheological properties, and its state of stress.

In this study we examine and discuss the nonlinear property of granular soils to undergo volumetric changes when sheared and its implication on seismic-wave propagation. First, the mechanism of dilatancy and contractancy is summarized from a soil mechanics point of view. Numerical calculations using a hypoplastic constitutive law, with which dilatancy can realistically be simulated, are performed for wave-propagation problems. We corroborate our thesis that P and S waves in cohesionless granular soils are coupled with laboratory experiments and analysis of earthquake seismograms.

Dilatancy and Contractancy: Nonlinear Properties of Granulates

Granular materials such as sands show peculiar behavior when subjected to shear deformations. Reynolds (1887) observed the tendency of soil to increase its volume under increasing deviatoric stress, which is known as dilatancy (Terzaghi and Peck, 1967). If no porosity changes occur during large strains, the sand is said to be at the critical void ratio (Casagrande, 1936).

When shearing an element of granular soil, the grain skeleton is reorganized, changing the volume (Fig. 1a). Shearing an initially loose and dry granulate with an angle γ shows hysteretic behavior (Fig. 1b) with contraction during the first cycles (Fig. 1c, solid line.) With repeated shear cycles the skeleton becomes denser, and the shear-stress ratio T_{12}/T_{11} increases sublinearly with increasing shearing angle γ (Fig. 1b,c, dashed lines). With sufficient shearing, the skeleton dilates, provided no grain crushing occurs, and T_{12}/T_{11} increases significantly. Granular soils always show initial contractant behavior, independent of its initial density

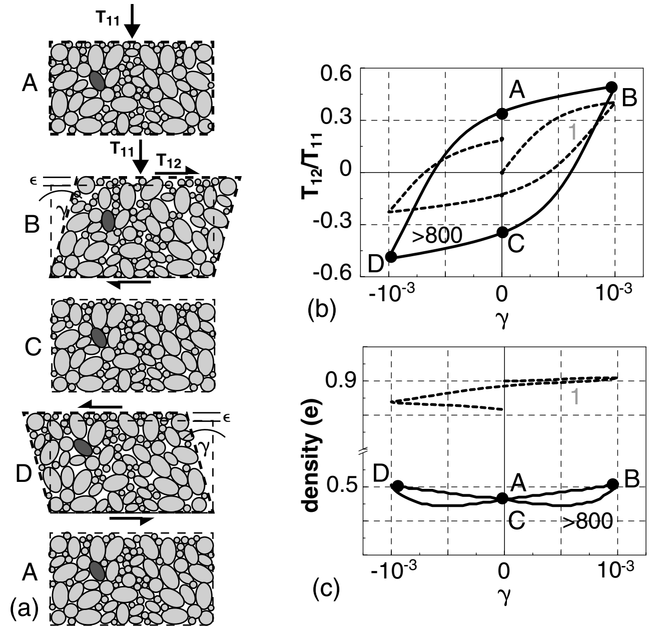

Figure 1. Schematic of a simple shear test showing dilatancy and contractancy with hysteresis, simulated using a hypoplastic material law. (a) A granular soil element is sheared by (b) angle γ, producing a extension ε perpendicular to shearing. Upon shear reversal, shear stress increases. Alternating shearing direction causes repeated dilation of the granular body. (c) During one shear cycle, the sand skeleton undergoes approx. two longitudinal volume changes Δe. T_{12}/T_{11} = shear-stress ratio; e = void ratio (porosity).

(Goldscheider, 1975), as shown in Figure 1c at the limit cycle.

Drnevich (1972) applied dynamic and quasi-static torsion on hollow cylindrical sand specimen to study pore pressure, shear modulus, and damping evolution as a function of initial conditions, strain amplitude, and number of cycles. He found that dilation caused a dynamic pore water pressure increase and that torsional vibration initiated longitudinal vibration, with the longitudinal frequency being exactly double the frequency of torsional oscillation. He attributed this observation to the dilatant property of sand. Resonant column experiments conducted by Huber (1998) on dry large ballast samples (diameter, 0.79 m; height, 0.84 m) also showed a peculiar frequency doubling. The gravel sample was subjected to a cyclic torque with a strain amplitude of $\gamma \cong 10^{-5}$. Tangential force F_t and acceleration a_t, as well as axial acceleration a_v, were measured. Acceleration time series show for the axial acceleration a_v a frequency twice the frequency of a_t with an amplitude ratio $a_v/a_t \approx 0.03$. (Fig. 2a).

Again, the underlying mechanism for this observed frequency doubling is contractancy and dilatancy, a characteristic of compressible grain skeletons (compared to incompressible granulates, e.g., when saturated). With dilatancy-induced frequency doubling being observed in dynamical

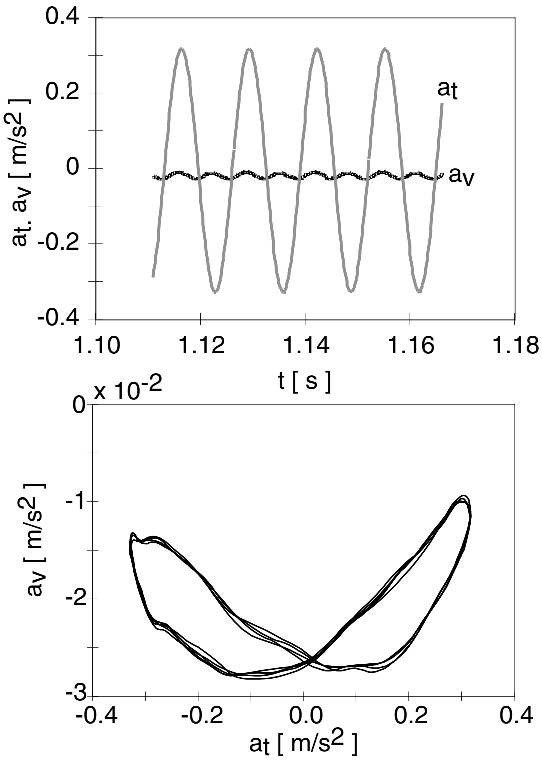

Figure 2. (a) Acceleration versus time acquired from a large resonant column experiment. Black line, vertical acceleration a_v; gray line, transversal acceleration *at*. (b) Phase diagram shows dilatancy and contractancy of ballast during tangential oscillation (Huber, 1998).

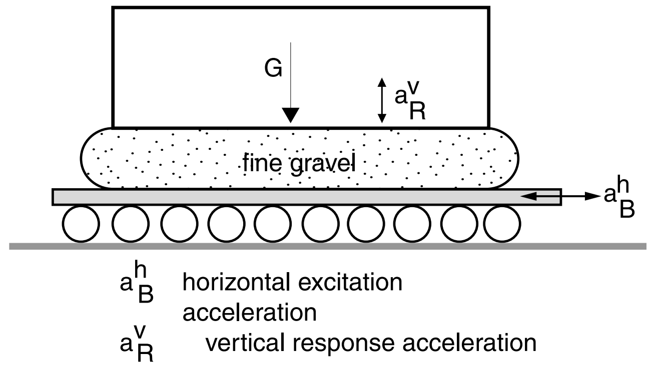

Figure 3. Sketch of the experiment setup of gravel-filled pillow on shaking table.

problems (Fig. 2b) the question that immediately suggests itself is whether this type of soil behavior can be induced through wave propagation.

Shaking Table Experiments

Experiments conducted on a shaking table investigating the behavior of noncohesive granular soils under seismic loading also show dispersive effects for medium-dense to dense granular soils. A pillow filled with almost saturated fine gravel and topped with a dead load was horizontally sheared at its base at various frequencies using a shaking table (Fig. 3). Horizontal and vertical accelerations were measured at the pillow base and its top. Figure 4 shows the horizontal base acceleration f_B^h time series and its frequency spectrum (gray). For purposes of emphasis, superposed is the spectrum for a specific 1-sec time window. Both spectra show a distinct peak at 10 Hz. Figure 5 depicts the vertical response acceleration time series f_R^v and its spectrum that shows a much greater width than its horizontal counterpart. It is approximately twice as wide and the peaks shifted toward higher frequencies; hence the *P*-wave spectrum was dispersed.

The peak frequency ratio f_R^v/f_B^h for the selected 1-sec time window is approximately 2. The frequency doubling during one shear cycle is even more convincingly shown in the phase diagram (Fig. 6). However, the dispersive signature of the *P*-wave spectra can be also recognized in the overall spectra. The frequency doubling was observed at all frequencies and amplitudes, which strongly suggests that this phenomenon is due to a soil property and not due to a system resonance frequency.

Numerical Modeling of *P*- and *S*-Wave Interaction in Granular Soils

With several differently setup experiments showing the same phenomenon, any constitutive law claiming to realistically model soil behavior ought to reproduce the experimental results. Goldberg (1960) was among the first to theoretically show the interaction between *P* and *S* waves in an elastic medium for large-amplitude seismic waves. His solution yielded the following results: (1) *P* and *S* waves couple, (2) *S* waves induce *P* waves, (3) the induced waves have a dominant frequency twice the *S*-wave frequency, (4) the induced *P* waves propagate ahead with *P*-wave velocity.

Large-amplitude wave propagation through dry sand was numerically modeled by Osinov (1998) based on a hypoplastic constitutive model (Gudehus, 1992; Kolymbas and Wu, 1993) showing that the wave-propagation speed depends on the direction of deformation, hence unveiling nonlinearity.

Granular sediments, however, already show nonlinear behavior at very small deformations such as $\varepsilon \approx 10^{-5}$ due to the mechanism of dilatancy and contractancy as shown by Huber (1998).

In this study, wave propagation for moderate wave amplitudes in a dry sand layer (Fig. 7) was numerically modeled using an extended hypoplastic model that includes a so-called intergranular strain δ (Niemunis and Herle, 1997)—an internal state variable that describes the deformation history of the soil.

In this material law the stiffness matrix (**M**) depends on

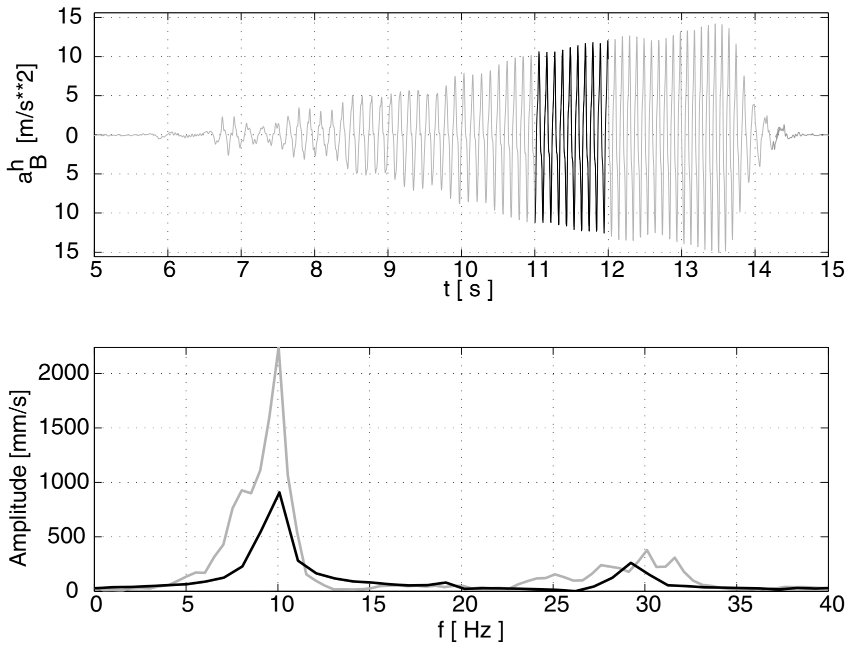

Figure 4. Horizontal excitation acceleration time series (top) and their spectral analyses (bottom) during shaking table experiments (gray). Black line shows time series and spectrum for a 1-sec window.

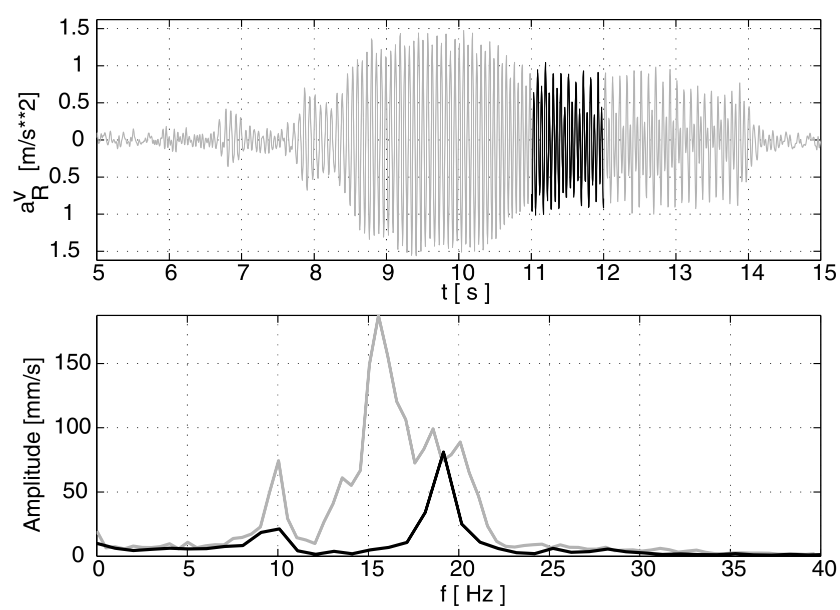

Figure 5. Complete vertical acceleration time series (top) and their spectral analyses (bottom) during shaking table experiments. Black line shows time series and spectrum for a 1-sec window.

the actual effective stress (**T**), the void ratio e, and δ (see equation 1)

$$\overset{0}{\mathbf{T}} = \mathbf{M}(\mathbf{T}, e, \delta) : \mathbf{D}, \tag{1}$$

where **D** is the stretching tensor, and $e = (V_g + V_l)/V_s$, void ratio; V_g, gas volume; V_l-liquid volume; V_s, solid volume. The elastic and plastic soil behavior depends on the value of the intergranular strain δ. When fully mobilizing δ (i.e., large amplitudes), the soil behavior can be described according to equation 2:

$$\overset{0}{\mathbf{T}} = \mathbf{L} : \mathbf{D} + \mathbf{N} \cdot \|\mathbf{D}\|. \tag{2}$$

The stretching tensor **D** has the components

$$D_{ij} = \frac{1}{2}\left(\frac{\partial v_i}{\partial x_j} + \frac{\partial v_j}{\partial x_i}\right),$$

and the term |**D**| couples the vertical and horizontal motion. This can be easily shown for the specific case of plane-wave propagation. The particle velocity field in this case depends only on depth and time: $v_p(z, t)$ for the vertical components and $v_s(z, t)$ for the horizontal components. For plane waves, |**D**| equals

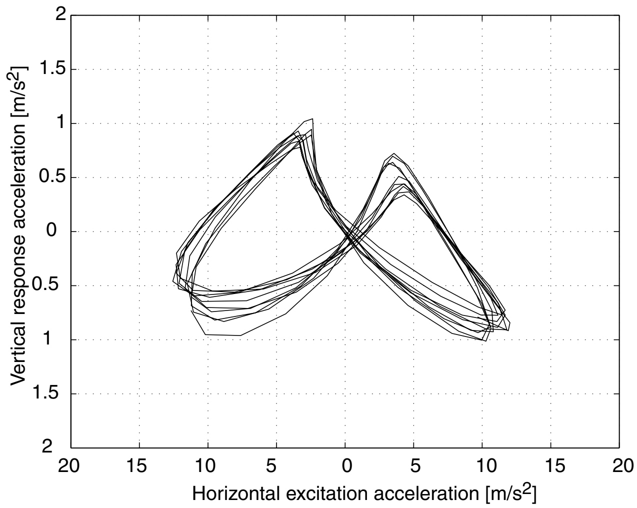

Figure 6. Phase diagram of acceleration data for a 1-sec window during shaking table experiments.

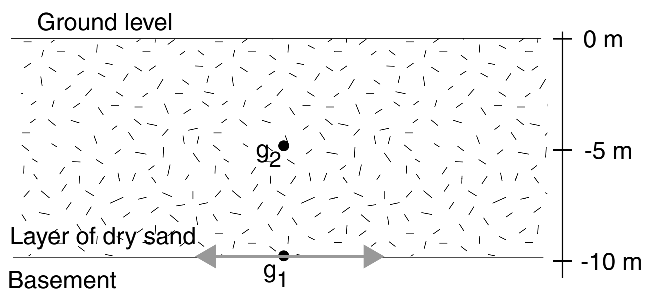

Figure 7. Schematic profile of sand layer for numerical modeling: g_1, numerical geophone at sand layer base; g_2, numerical geophone in the center of layer; v_P, longitudinal particle velocities of first arrival; v_S, transversal particle velocities; v_Δ, particle velocities of dilatancy-induced Δ wave.

$$\sqrt{\left(\frac{\partial v_p}{\partial z}\right)^2 + 0.5\left(\frac{\partial v_s}{\partial z}\right)^2},$$

showing the coupling of P and S waves for deformations larger than, say, $\varepsilon \approx 10^{-5}$. Figure 8 shows the numerical boundary condition for a shear-wave excitation at the base of a sand layer of 10-m thickness at hydrostatic state (Figure 7). Dominant excitation frequency was 4 Hz with an amplitude of 5 cm/sec, which amounts to a moderate seismic event with a shear deformation of $\varepsilon \approx 3 \times 10^{-4}$. As the S wave propagates upward, particle velocities are not altered much. In fact, lacking amplitude attenuation or even its amplification is consistent with decreasing pressure. The frequency content remains more or less constant, for example, for a midpoint in the sandlayer (Fig. 9). On this wave path, Δ waves were induced with approximately double frequency (Fig. 10) due to the dilatancy mechanism explained previously.

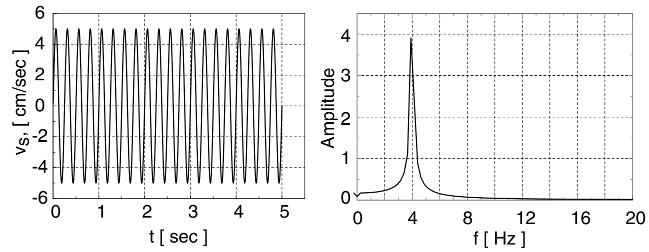

Figure 8. Boundary condition for numerical simulation. Shown are horizontal particle velocities versus time and their spectrum at sand layer base (Fig. 7,g_1). Thickness of dry sand layer is 10 m, and its average density is $\tilde{\rho} \approx 1.65 \cdot 10^3$ kg/m^3 (resulting in a void ratio of $e = 0.6$). Hydrostatic initial stress distribution with 0 kPa at the surface and 165 kPa at the base.

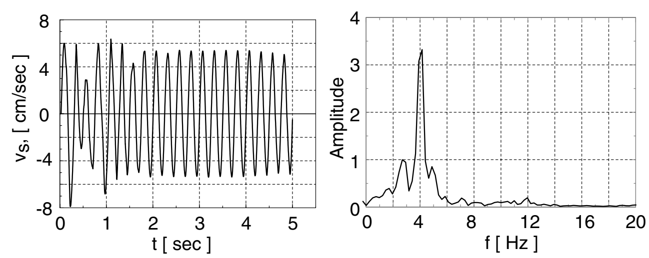

Figure 9. Horizontal particle velocities versus time and their spectrum at midpoint of sand layer (see Fig. 7, g_2).

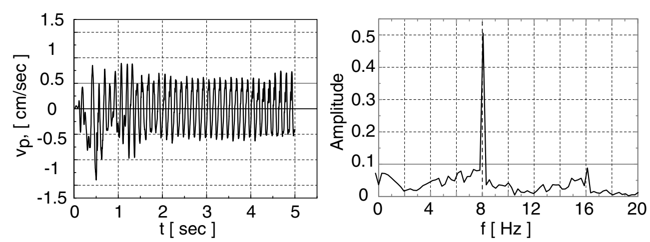

Figure 10. Vertical particle velocities versus time and their spectrum at midpoint of sand layer (see Fig. 7, g_2).

A P-wave predominant frequency shift toward twice the S-wave frequency was analytically shown by Gottlieb and Loukachev (1998) and Loukachev (2002).

The amplitude of the Δ wave reaches for this case 8% of the horizontal source wave amplitude. The Δ-wave amplitude is not constant because dilatancy and contractancy is a function of the void ratio e (porosity) and the average grain pressure (Gudehus, 1981). The Δ wave is approximately twice as fast as the S wave.

Seismogram Analysis with Regard to Dilatancy-Induced Dispersion

The experimental and numerical results shaped the hypothesis that dispersive signatures in *P*-wave spectra could be the result of *S*-wave-induced longitudinal Δ waves. Hence, accelerograms from two moderate earthquakes recorded at three stations in the seismically very active Vrancea Region (Romania) were analyzed. Data were provided from one soil station (INC) and two hard-rock stations (CFR and VID). The earthquake magnitudes (M_w) were 4.1 and 4.6. Table 1 summarizes the geologic setting of the recording stations whose data were used for this study.

Figure 11a–c shows the unfiltered accelerograms time series and their smoothed frequency spectra for two earthquakes, November and December 1997, for each station. The spectral analysis was performed on the complete time series, and smoothing was performed using a time window of 100 msec (stations INC and VID) and 150 msec (station CFR), respectively.

Frequency spectra from rock and soil stations are compared. It can be seen that the rock-station data do not show any major differences between the frequency ranges of *P* and *S* waves. On the other hand, the *P*-wave spectra of the soil station show a significant dispersion toward higher frequencies with maxima approximately twice the shear-wave peak frequency. This dispersion can be explained by the mechanism of dilatancy and contractancy, provided the soil allows for volumetric changes, which is only possible if granular layers show a degree of saturation lower than 1.

Table 1
Geologic Setting of Stations Providing Accelerograms for This Study*

Station Name (subsurface type)	Geology
INC (soil)	Quaternary gravel, sand and sandy clay, clay and loess (350–400 m) Upper Neogene clays, sands, sandy clays and marls with chalky layerings (600–650 m) Cretaceous limestone basement at ca. 1000 m
CFR (rock)	slate, quartzitic and limey sandstone, limestone Silurian and Lower Devonian (down to 500–1000 m)
VID (rock)	gneiss down to 4000 m, some mica schist

*Data provided by Fielitz (2000, personal comm.).

Discussion and Conclusions

Based on numerical, experimental, and field investigations, this study suggests that dispersion observed in the *P*-wave spectra can be attributed to the dynamic interaction of *S* and *P* waves in granular soils. Transverse waves of a given amplitude propagating through granular soils induce volume changes owing to the dilating nature of granulates with a density below critical, which manifest themselves as longitudinal, so-called Δ waves. The Δ-wave frequency is approximately double that of the transversal source wave. A hypoplastic constitutive relation has been verified for various initial boundary problems and models the observed dispersion well. *P* waves propagate ahead of *S*-waves producing a first-arrival signature on a seismogram. As soon as an *S* wave with its specific frequency content enters the base of a compressible granular layer, it continuously induces Δ waves. The Δ-wave spectrum will be superposed onto the first-arrival *P*-wave spectrum, causing a dispersion as a particular signature. The *P*-wave peak frequency is approximately double that of the *S* wave. Since *S* waves, depending on the hypocentral distance, can arrive significantly later than *P* waves—according to Wenzel *et al.* (1998) the travel-time difference between *P* and *S* waves amounts to 25 sec for the Bucharest region—one would expect a time lag $t_s - t_\Delta$ between the first arrivals of the *P* and Δ waves to be indicative of the thickness of the dilative granular layer.

However, this is not observed. The *P*-wave spectra show a greater width than the *S*-wave spectra also for incremental successive time windows. This can be explained with the transversal components of the *P* wave immediately inducing Δ waves before the *S* waves even reach the dilative layer.

Numerous studies clearly show evidence of nonlinear soil behavior when comparing mainshock to aftershock data, for example, Beresnev and Wen (1996), Field *et al.*, (1998), Beresnev and Wen (1995), attributing nonlinearity to the hysteretic behavior of soils at large deformations. However, in those approaches, seismic responses carrying specific information owing to the particular station are obliterated due to averaging processes. Other authors filtered the time series (Bonjer *et al.,* 1999) or explained the observed generation of *P* waves as a result of *SV* conversion (Takahashi *et al.,* 1992). The notorious disregard for *P*-wave analyses (or their filtering) has prevented earlier insight with regard to the interaction of *P* and *S* waves. The results presented show that nonlinear soil behavior (1) has different facets and (2) is apparently not restricted to a comparison between strong- and weak-motion events.

Dilatancy and contractacy, which are characteristics of granular soils, can explain a peculiar fingerprint on the *P*-wave spectra, which is not only observed for *P* waves of moderate earthquakes, but can also be reproduced in laboratory shaking table and resonant column experiments.

Furthermore, evaluating seismograms also with respect to Δ waves may provide a useful tool for acquiring additional subsurface information of individual loci because soil allowing for volume changes are not fully saturated—a piece of information essential for microzonation.

Acknowledgments

This work was supported by the Collaborative Research Programme (SFB 461). We gratefully acknowledged Prof. Lungu from the Technical University for Constructions, Bucharest, and the Geophysical Institute of

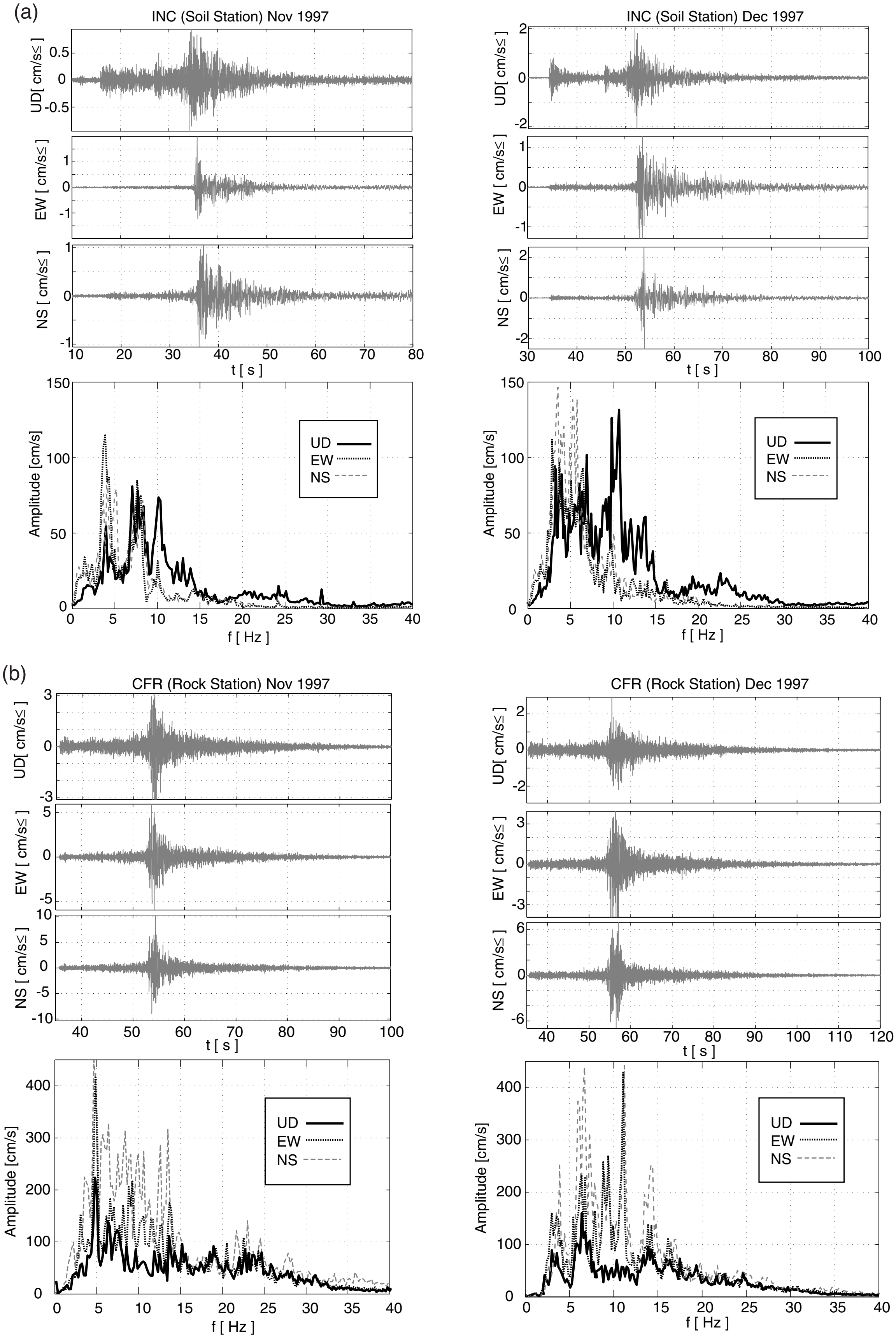

Figure 11. Caption on facing page.

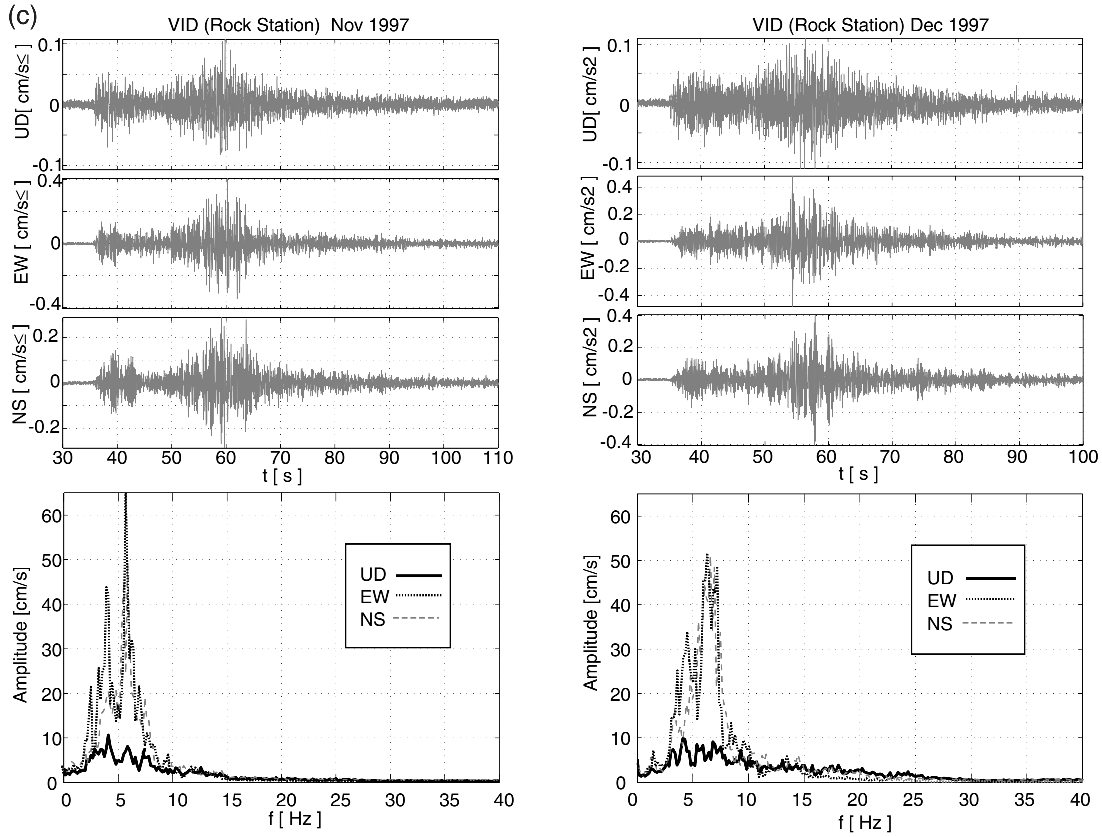

Figure 11. (a) Ground-motion accelerograms and their smoothed spectral analysis from two earthquakes recorded at soil station INC. Each spectrum shows both horizontal components (north–south, east–west) and the vertical component (up–down). *P*-wave spectra of the soil station are broader, with its frequency range being approximately twice as wide as the *S*-wave spectra. (b) Ground-motion accelerograms and their smoothed spectral analysis from two earthquakes recorded at rock station CFR. Each spectrum shows both horizontal components (north–south, east–west) and vertical component (up–down). When comparing the spectra from rock stations they show a similar frequency range for *S* and *P* waves. (c) Ground-motion accelerograms and their smoothed spectral analysis from two earthquakes recorded rock station VID. Each spectrum shows both horizontal components (north–south, east–west) and vertical component (up–down). When comparing the spectra from rock stations they show a similar frequency range for *S* and *P* waves.

the University of Karlsruhe for providing earthquake data from Romania. We are grateful to the anonymous reviewers for the valuable remarks.

References

Aki, K. (1993). Local site effects on weak and strong ground motion, *Tectonophysics* **218,** 93–111.

Bard, P.-Y. (1994). Effects of surface geology on ground motion: recent results and remaining issues, in *Quelle: 10th European Conference on Earthquake Engineering 1994,* Duma (Editor), Vienna, Austria.

Belyakov, A. S., A. G. Gamburtsev, V. S. Lavrov, A. V. Nikolaev, and N. K. Privalovskii (1996). Vibration action on rocks and their induced seismic emission, *Izvestiya, Phys. Solid Earth* **32,** no. 2, 149–155.

Beresnev, I. A., and A. V. Nikolaev (1988). Experimental Investigation of Nonlinear Seismic Effects, *Phys. Earth Planet. Interiors* **50,** 83–87.

Beresnev, I. A., and K. L. Wen (1995). P-wave amplification by near-surface deposits at different excitation levels, *Bull. Seism. Soc. Am.* **85,** 1490–1494.

Beresnev, I. A., and K. L. Wen (1996). Nonlinear soil response: a reality? *Bull. Seism. Soc. Am.* **86,** no. 6, 1964–1978.

Beresnev, I. A., E. H. Field, K. V. Den Abeele, and P. A. Johnson (1998). Magnitude of nonlinear sediment response in Los Angeles basin during the 1994 Northridge, California, Earthquake, *Bull. Seism. Soc. Am.* **88,** no. 4, 1079–1084.

Beresnev, I. A., A. V. Nikolaev, V. S. Solov'ev, and G. M. Shalashov (1986). Nonlinear phenomena in seismic surveying using periodic vibrosignals, *Izvestiya, Earth Phys.* **22,** no. 10, 804–811.

Beresnev, I. A., K.-L. Wen, and Y. T. Yeh (1994). Seismological evidence for nonlinear elastic ground behaviour during large earthquakes, *Soil Dyn. Earthquake Eng.* **14,** 103–114.

Beresnev, I. A., K.-L. Wen, and Y. T. Yeh (1995). Nonlinear soil amplification: its corroboration in Taiwan, *Bull. Seism. Soc. Am.* **85,** no. 2, 496–515.

Bernatzik, W. (1947). *Baugrund und Physik*, Schweizer Druck und Verlagshaus, Zürich.

Bolt, B. A. (1995). *From Earthquake Acceleration to Seismic Displacement,* Wiley & Sons, New York.

Bonjer, K. P., M.-C. Oncescu, and L. Driad (1999). A note on empirical site responses in Bucharest, Romania, in *Vrancea Earthquakes: Tectonics, Hazard and Risk Mitigation,* I. Wenzel, D. Lunga, O. Novak (Editors), Kluwer Academic Publishers, Dordrecht, 27–42.

Casagrande, A. (1936). Characteristics of cohesionless soils affecting the stability of slopes and earth fills, *J. Boston Soc. Civil Eng.* **23,** no. 1, 13–32.

Castro, G. (1969). Liquefaction of sands, *Ph.D. Thesis,* Harvard University, Cambridge, Massachusetts.

Chin, B.-H., and K. Aki (1991). Simultaneous study of the source, path, and site effects on strong ground motion during the 1989 Loma Prieta Earthquake: a preliminary result on pervasive nonlinear site effects, *Bull. Seism. Soc. Am.* **81,** no. 5, 1859–1884.

Darragh, R. B., and A. F. Shakal (1991). The site response of two rock and soil station pairs to strong and weak ground motion, *Bull. Seism. Soc. Am.* **81,** no. 5, 1885–1899.

Dimitriu, P., I. Kalogeras, and N. Theodulius (1999). Evidence of nonlinear site response in horizontal-to-vertical spectral ratio from near-field earthquakes, *Soil Dyn. Earthquake Eng.* **18,** 423–435.

Dimitriu, P., N. Theodulidis, and P.-Y. Bard (2000). Evidence of nonlinear site response in HVSR from SMART1 (Taiwan) data, *Soil Dyn. Earthquake Eng.* **20,** 155–165.

Drnevich, V. P. (1972). Undrained cyclic shear of saturated sand, *J. Soil Mech. Found. Div. ASCE* **98,** no. SM8, 807–825.

Field, E. H., P. A. Johnson, I. A. Beresnev, and Y. Zeng (1998). Nonlinear ground-motion amplification by sediments during the 1994 Northridge earthquake, *Nature* **390,** 599–602.

Goldberg, S. A. (1960). About interaction of longitudinal and transversal elastic waves, *Acoustic Journal* **VI,** no. 3, 307–310 (in Russian).

Goldscheider, M. (1975). Dilatanzverhalten von Sand bei geknickten Verformungswegen, *Mech. Res. Comm.* **2,** 143–148.

Gottlieb, J., and I. Loukachev (1998). Nonlinear wave propagation in soil: modelling of a special phenomenon and identification of parameters, in *Proc. 4th Int. Conference on Mathematical and Numerical Aspects of Wave Propagation,* Colorado School of Mines, Golden, Colorado, 679–681.

Gudehus, G. (1981). *Bodenmechanik,* Enke Verlag, Stuttgart.

Gudehus, G. (1992). A comprehensive constitutive equation for granular materials, *Soils Found* **36,** no. 1, 1–12.

Gudehus, G., I. Loukachev, and N. Pralle (2001). Inelastic behaviour of grain skeletons with propagation of plane shear waves, in *Int. Conf. of Powders and Grains,* Sendai, Japan, May 2001, Y. Kishino (Editor), Swets & Zeitlinger, A. A. Balkema, Rotterdam, The Netherlands, 125–128.

Heitz, J. F., and F. J. Sánchez-Sesma (1989). Nonlinear seismic response of a soft soil layer using a perturbation approach, in *Proc. 4th Int. Conf. on Soil Dynamics and Earthquake Engineering,* A. S. Cakmak (Editor), Mexico City, Mexico, 117–130.

Huber, G. (1998). Dynamisches Schotterverhalten in Resonanzsäulenversuch, VDI-Bahn-Baufachtagung, Berlin, 28–30 October.

Jarpe, S. P., C. H. Cramer, B. E. Tucker, and A. F. Shakal (1988). A comparison of observations of ground response to weak and strong ground motion at Coalinga, California, *Bull. Seism. Soc. Am.* **78,** no. 2, 421–435.

Johnson, P. A., T. J. Shankland, R. J. O'Connell, and J. N. Albright (1987). Non-linear generation of elastic waves in crystalline rock, *J. Geophys. Res.* **92,** no. B5, 3597–3602.

Kolymbas, D., and W. Wu (1993). Introduction to hypoplasticity, in *Modern Approaches to Plasticity,* D. Kolymbas (Editor), Elsevier, Amsterdam, 213–223.

Loukachev, I. (2002). Dilatanzwellen und Schichttrennung bei Wellenansbreitung in Sandigen Böden, *Ph.D Thesis,* Department of Soil and Rock Mechanics, University of Karlsruhe, Karlsruhe, Germany (in press) (in German).

Loukachev, I., N. Pralle, and G. Gudehus (2000). Starkbebenwellen in Granulatschichten, in *Beiträge zum Workshop in Bochum "Boden unter fast zyklischer Belastung: Erfahrungen und Forschungsergebnisse,"* Th. Triandifyllidis (Editor), Schriftenreihe des Institutes für Grundbau und Bodenmechanik der Ruhr-Universtität Bochum, Heft 32, 21–38.

Niemunis, A., and I. Herle (1997). Hypoplastic model for cohesionless soils with elastic strain range, *Mech. Cohesive-Frictional Mat.* **2,** 143–148.

Nikolaev, A. V. (1988). Problems of nonlinear seismology, *Phys. Earth Planet. Interiors* **50,** 1–7.

Osinov, V. (1998). Theoretical investigation of large-amplitude waves in granular soils, *Soil Dyn. Earthquake Eng.* **1,** no. 17, 13–28.

Pease, J. W., and T. D. O'Rourke (1997). Seismic response of liquefaction sites, *J. Geotech. Geoenviron. Eng. ASCE* **123,** no. 1.

Reynolds, O. (1887). Experiments showing dilatancy, a property of granular material, possibly connected with gravitation, *Proc. R. Inst.* 354–363.

Sato, K., T. Kokusho, M. Matsumoto, and E. Yamada (1996). Nonlinear seismic response and soil property during strong motion, in *Special Issue of Soils and Foundations,* No. 1, Japanese Geotechnical Society, 41–52.

Solovev, V. (1990). Experimental investigation on nonlinear seismic effects, *Phys. Earth Planet. Interiors* **6,** 271–276.

Studer, J. A., and M. G. Koller (1997). *Bodendynamik*, Second Ed., Springer Verlag, Berlin.

Suetomi, I., and N. Yoshida (1998). Nonlinear behaviour of surface deposit during the 1995 Hyogoken-Nambu earthquake, in *Special Issue of Soils and Foundations,* No. 2, Japanese Geotechnical Society, 11–22.

Takahashi, K., S. Ohno, M. Takemura, T. Ohta, Y. Sugawara, T. Hatori, and S. Omote (1992). Observation of earthquake strong motion with deep borehole generation of vertical motion propagating in surface layer after S-wave arrival, in *Proc. 10th World Conference of Earthquake Engineering,* Vol. 3, 1245–1250.

Terzaghi, K. (1925). *Erdbaumechanik auf bodenphysikalischer Grundlage*, Deuticke Verlag, Leipzig und Wien.

Terzaghi, K., and R. B. Peck (1967). *Soil Mechanics in Engineering Practice,* Wiley & Sons, New York.

Wen, K.-L., I. A. Beresnev, and Y. T. Yeh (1994). Nonlinear soil amplification inferred from downhole strong seismic motion data, *Geophys. Res. Lett.* **21,** no. 24, 2625–2628.

Wenzel, F., M. Baur, M. C. Oncescu, F. Fiedrich, and C. Ionescu (1999). 25 Seconds for Bucharest, in *Vrancea Earthquakes,* F. Wenzel *et al.* (Editors), Kluwer Academic Publishers, Dordrecht.

Yang, J., T. Sato, and L. Xiang-Song (2000). Nonlinear site effects on strong ground motion at a reclaimed island, *Can. Geotech. J.* **37,** 26–39.

Yu, G., J. G. Anderson, and R. Siddharthan (1992). On the characteristics of nonlinear soil response, *Bull. Seism. Soc. Am.* **83,** no. 1, 218–244.

Institute of Soil & Rock Mechanics
University of Karlsruhe
P.O. Box 6980
D-76128 Karlsruhe, Germany
louka@ibf-tiger.bau-verm.uni-karlsruhe.de
pralle@ibf-tiger-bau-verm.uni-karlsruhe.de
gudehus@ibf-tiger.bau-verm.uni-karlsruhe.de

Manuscript received 15 February 2001.

View publication stats